42nd AIAA/ASME/SAE/ASEE Joint Propulsion Conference & Exhibit
9 - 12 July 2006, Sacramento, California

AIAA 2006-4993

The Magnetic Interference Hall Accelerator

Cliff Thomas*, Emmanuelle Sommier†, Nicolas Gascon‡, and Mark Cappelli§
Stanford University, Stanford, CA, 94305-3032, United States

This paper introduces a new concept for the magnetic field in a Hall-effect thruster. The Magnetic Interference Hall Accelerator (MIHA) uses independent magnetic circuit elements to put its peak magnetic field outside its exit plane. As a result, the zone of minimum electron mobility is outside its exit plane, as well as its ion acceleration zone. Wall-effects are reduced, and ion bombardment of the channel wall is moderated. The design and operating behavior of a MIHA prototype is detailed, and thrust is determined at several operating conditions. The plasma potential is measured, and verifies an external acceleration zone.

Nomenclature

Φ	Potential (V)
$\mathbf{E}$	Electric Field (V/m)
$\mathbf{B}$	Magnetic Field (T)
$\mathbf{I}$	Current (A)
$\mathbf{R}$	Position (m)
μ_o	Magnetic Permeability (N/A^2)
k_b	Boltzmann Constant (J/K)
n_α	Number Density (m^{-3})
c_α	Thermal Velocity (m/s)
q_α	Charge (C)
m_α	Mass (kg)
T_α	Temperature (K)

I. Introduction

The closed-drift Hall plasma accelerator, or Hall-effect thruster (HET), has been in use since the early 1970s for high specific impulse satellite propulsion.[1] In the Hall thruster, ion acceleration is achieved between an anode and a hot-emitting cathode by an electrostatic field, $\mathbf{E}$, and electron motion is impeded by an applied orthogonal magnetic field, $\mathbf{B}$ (see Fig. 1). The discharge is coaxial, so electrons execute closed-drift motion in the azimuthal direction ($\mathbf{E} \times \mathbf{B}$). Because of their mass, the ions can move freely, and obtain an energy determined by their point of ionization in the potential field. In most Hall thrusters, the ions ultimately carry $70 - 90\%$ of the discharge current depending on the effectiveness of the design at inhibiting electron migration.

Classical diffusion theory (which scales as B^{-2}) underestimates the transport of electrons in the HET, and numerical models of the discharge must commonly invoke an anomalous diffusion coefficient (like that of Bohm, varying as B^{-1}) to achieve acceptable results.[2] An analysis by Fife[3] of early Russian experimental results,[4] and recent measurements at Stanford,[5,6] indicate the electron mobility (which is proportional to the inverse Hall parameter, $(\omega\tau)^{-1}$) is a strong function of position. In some portions of the discharge, the

*Research Assistant, Mechanical Engineering Department, Building 520, Student Member.
†Research Assistant, Mechanical Engineering Department, Building 520, Student Member.
‡Research Associate, Mechanical Engineering Department, Building 520, Regular Member.
§Professor, Mechanical Engineering Department, Building 520, Regular Member.

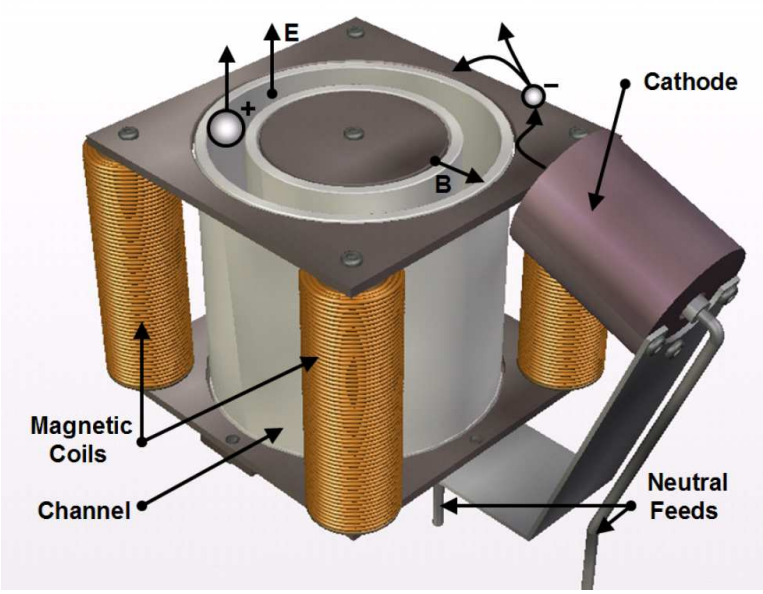

Figure 1. Diagram of a Hall-effect thruster.

inverse Hall parameter is close to the Bohm value, $(\omega\tau)^{-1} = 1/16$.[7] However, in those regions where the magnetic field is strongest, the mobility approaches the value expected for classical diffusion. The reason for this behavior is a subject of debate,[8,9] but it is usually attributed to fluctuations in the potential and/or electron-wall interactions. In either case, anomalous transport mechanisms cause the electron current to exceed its classical value.

Anomalous transport reduces the thrust efficiency of the Hall-effect thruster; it reduces the ion current fraction. Less obvious though, is its impact on the Hall thruster's operational life. The Ion Energy Distribution Function (IEDF) is determined by the electrostatic potential, and again, the electron mobility. As a consequence, it is difficult to predict the rate that ions will collide with the ceramic channel. Since high-energy ion bombardment limits the life of the HET, it is difficult to design for increased life. Furthermore, optimizing for increased life is made more difficult by the location of the peak **B**. In the conventional Hall accelerator, the ion acceleration zone is near the peak magnetic field. Due to the design of the magnetic circuit, the peak magnetic field is inside the ceramic channel or very near its exit. As a result, it is guaranteed that high-energy ions will impact the channel wall and limit the life of the conventional Hall accelerator.

This paper describes a concept for the magnetic field in the Hall-effect thruster that could simplify anomalous transport, reduce erosion due to ion bombardment, and lead to improved Hall thruster design. The Magnetic Interference Hall Accelerator, MIHA, pushes the minimum electron mobility outside the channel. As a result, the ion acceleration zone is outside the channel. Since the discharge is sustained in vacuum, high-energy ion bombardment of the ceramic channel is moderated, and electron-wall interactions are reduced. Since the electron mobility is "simplified", the design could allow for greater optimization of the magnetic field. The MIHA magnetic circuit is discussed, as well as a prototype design. The prototype is found to operate like a conventional Hall accelerator, and display several typical behaviors: the "breathing mode" oscillation at moderate discharge power, an increase in the discharge current with an increase in voltage, and a decrease in discharge current with an increase in the magnetic field. Unlike a conventional accelerator though, the wall material has a weak impact on the discharge. To demonstrate our findings, the general operating characteristics of a prototype MIHA thruster are detailed. Current-voltage characteristics, discharge current fluctuation spectra, and thrust measurements are provided. To demonstrate the movement of the acceleration zone to a point outside the exit plane, plasma potential measurements are provided.

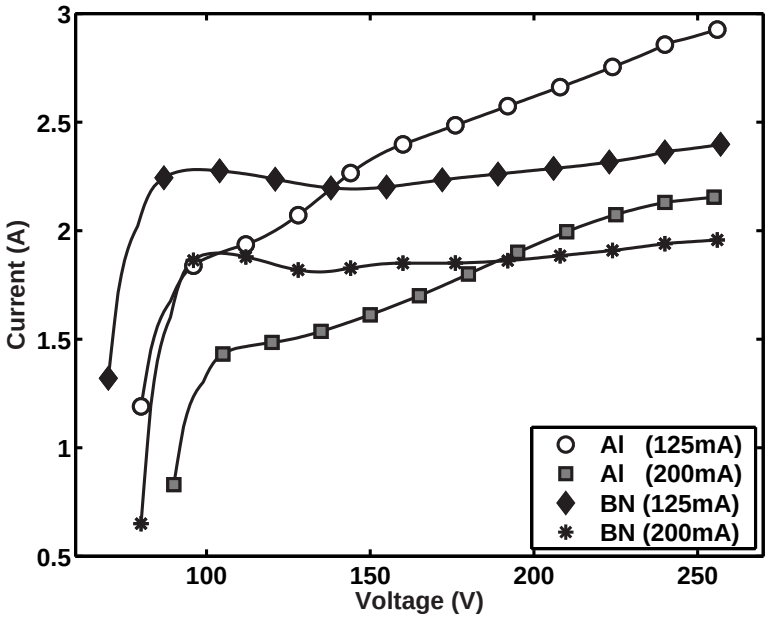

Figure 2. Current-voltage characteristics for the Stanford SPT.

II. The MIHA Concept

A. An Experimental Motivation

Previous experiments have demonstrated the importance of the channel wall material (and by implication, electron-wall interactions) on the behavior of the conventional Hall accelerator (see Fig. 2).[9,10] In fact, the observed dependence is the basis for near-wall conductivity theory - the idea that electron-wall interactions determine the electron mobility. Near-wall conductivity assumes that hot electrons (electrons with kinetic energy greater than the sheath potential) pass through the sheath, scatter, and contribute to transport. This phenomena is difficult to quantify though, because the high-energy electron population is difficult to estimate. This is because the wall scattering function (including the secondary electron emission coefficient) is uncertain for most wall materials, and unknown for others. Since the population of hot electrons is a sensitive function of electron-wall scattering, even a small error in its value can cause similar simulations to give divergent results. As it is, the relevance of near-wall conductivity is not agreed on.[8,9]

The plausibility of near-wall conductivity is made more uncertain though, since plasma fluctuations can account for some portion of the observed transport.[11] Furthermore, theoretical findings have demonstrated that for some materials, the population of hot electrons is insufficient to account for the observed mobility.[8] Finally, near-wall conductivity makes no attempt to explain transport past the exit plane. Since it is understood though, that the channel wall material impacts the discharge in the conventional Hall accelerator, it may or may not be responsible for the observed electron mobility, and its total effect is difficult to predict or quantify, it has been speculated whether a change in the Hall-effect thruster could reduce the impact of the wall, lead to improved performance, or provide greater discharge predictability. Experiments hint at this possibility.[12]

In a previous study, we have operated the Stanford Linear Thruster (SLT), whose wall material could easily be changed.[12] The aim of the study was to demonstrate the importance of wall material, and to demonstrate the feasibility of CVD diamond as the channel wall material in a Hall-effect thruster. Unexpectedly, it was found that the wall material *did not* have a significant impact on the SLT, and its current-voltage behavior demonstrated less structure than previous measurements (see Fig. 3).

The mechanism responsible for this finding was initially uncertain, but given later LIF data, an intriguing hypothesis is readily made. Ion acceleration is accomplished *outside* the discharge channel in the SLT (see Fig. 4), whereas for most thrusters, the ion acceleration zone is *inside* the channel. As a consequence, it can be assumed that the minimum electron mobility, the peak electric field, and the acceleration zone, are

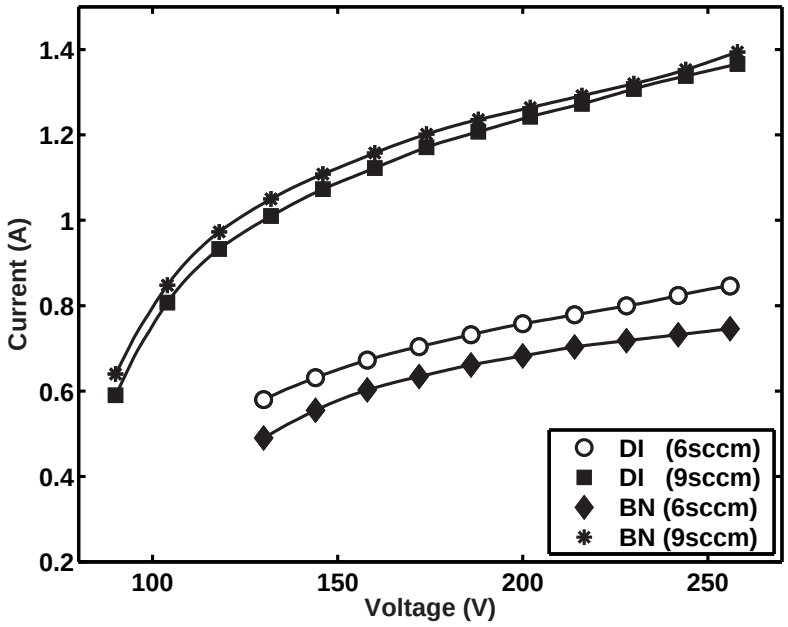

Figure 3. Current-voltage characteristics for the Stanford Linear Thruster.

outside the exit plane of the SLT. Since the primary physics of the discharge occur in vacuum, it is easy to understand why the wall material plays a weak role; the discharge is not confined by a material boundary. Naturally, this raises the question of why the electron mobility is so high in the channel, given that the peak **B** has been measured to be *inside* the channel. At present, two possibilities suggest themselves, but neither has been experimentally verified. First, the peak magnetic field is measured in vacuum, though the peak magnetic field including self-induction could be outside the channel. This is thought to be unlikely though, since a previous study in the Stanford SPT only demonstrated a shift in the peak magnetic field due to self-induction of $2-5$mm.[13] Since the minimum electron mobility in the SLT (which should be correlated to the maximum magnetic field) is $1-2$cm outside the SLT - self-induction is an unlikely explanation. The second possibility, and the one thought to be more likely, is that linear-geometry Hall accelerators are characterized by high mobility within their channel. As a result, the minimum electron mobility, the peak **E**, and the body of the discharge in this type of thruster are outside their channel, and wall-effects are reduced.

Since wall-effects play a diminished role in the SLT, it is likely that the discharge can be accurately modelled using a fluctuation-induced transport theorem,[14] Bohm transport,[7] or neoclassical transport. This exercise has not been completed though, since more data is needed. Also, since ion acceleration is outside the channel, ion bombardment is reduced, and increased life could result. For these reasons, a second linear thruster was made (with the expectation of external acceleration) to look for verification of the previous results,[12] and to test a magnetic field configuration designed for external acceleration.

The new thruster, MIHA, was designed to work more naturally with an external acceleration zone. In the SLT, the magnetic field was made to decrease monotonically after the exit plane - throughout the acceleration zone - unlike the magnetic field in a conventional Hall accelerator (which is shaped like a Gaussian). Since it is understood that poor efficiency can result from a negative-only gradient in **B**,[15] a magnetic field geometry was chosen to place the peak magnetic field outside MIHA, to allow a positive gradient in the magnetic field leading up to the acceleration zone, and give the magnetic field a more Gaussian profile. Lastly, a "top" stage was included to test the mobility inside the discharge channel - to determine whether a high mobility within the channel could explain external acceleration (if observed).

B. To Position The Magnetic Field

The idea of placing the peak magnetic field outside the exit plane of a Hall accelerator is not new. Previous magnetic circuit designs have put the peak magnetic field $1-2$mm outside the exit. To the knowledge of the authors, this was done to reduce erosion. A new design was needed though, to place the

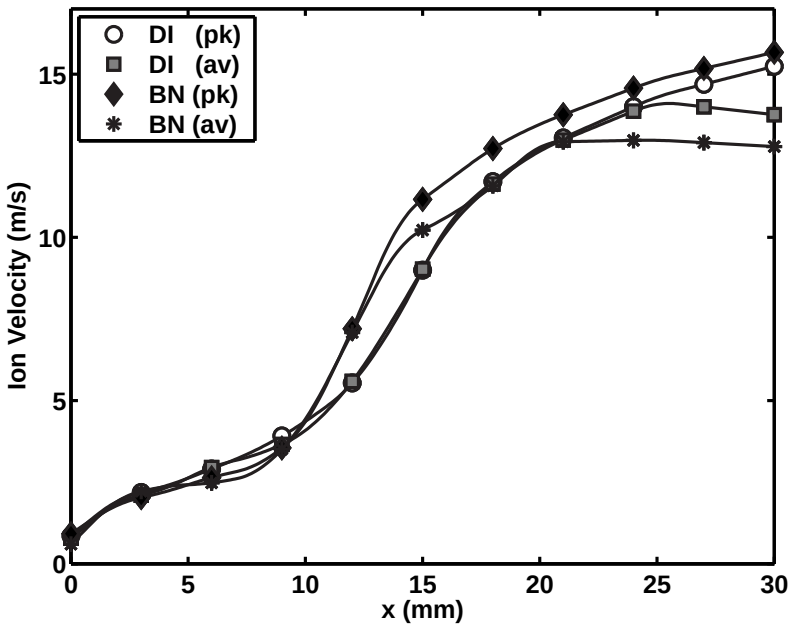

Figure 4. Ion velocity profile for the Stanford Linear Thruster.

peak magnetic field $1-2$cm outside the exit plane, so the resulting magnetic field profile might match with an external acceleration zone (see Fig. 4). To accomplish this, the Magnetic Interference Hall Accelerator concept, MIHA, was developed. In MIHA, the magnetic field is the interference-field of multiple independent magnetic circuit elements. By careful positioning of the circuit elements, the peak magnetic field is arbitrarily positioned.

The MIHA concept is demonstrated by a simple example in 2D - the interference-field of two parallel line currents. If the line currents are defined as $\mathbf{I_1}$ and $\mathbf{I_2}$ (in the $\mathbf{z}$ direction), and are located at position $\mathbf{R_1}$ and $\mathbf{R_2}$, respectively, the magnetic field in the $\mathbf{x}-\mathbf{y}$ plane due to either is easily calculated (see Eq. (1) and Eq. (2)).

$$\mathbf{B_1} = \left(\frac{\mu_o}{2\pi}\right)\left(\frac{\mathbf{I_1}\times(\mathbf{R}-\mathbf{R_1})}{|\mathbf{R}-\mathbf{R_1}|^2}\right) \tag{1}$$

$$\mathbf{B_2} = \left(\frac{\mu_o}{2\pi}\right)\left(\frac{\mathbf{I_2}\times(\mathbf{R}-\mathbf{R_2})}{|\mathbf{R}-\mathbf{R_2}|^2}\right) \tag{2}$$

Now, if special choices are made for the value and position of $\mathbf{I_1}$ and $\mathbf{I_2}$, we can force an interesting form for the total magnetic field, $\mathbf{B_T} = \mathbf{B_1} + \mathbf{B_2}$, on the $\mathbf{y} = 0$ line. If $\mathbf{I_1}$ and $\mathbf{I_2}$ have the same value, I, have the same position in $\mathbf{x}$, r_x, and are in opposite positions in $\mathbf{y}$, $\pm r_y$, the total magnetic field on the $\mathbf{y} = 0$ line is given by Eq. (3).

$$\mathbf{B_T} = \left(\frac{\mu_o I}{\pi}\right)\left(\frac{(\mathbf{x}-r_x)}{(r_y)^2+(\mathbf{x}-r_x)^2}\right)\hat{\mathbf{y}} \tag{3}$$

Eq. (3) is interesting, since the magnetic field is $\hat{\mathbf{y}}$ only, is zero when $\mathbf{x} = r_x$, and approaches zero as $\mathbf{x}\to\infty$ (implying maxima or minima in $\mathbf{B_T}$ at finite $\mathbf{x}$). Solving for $\nabla_{\mathbf{x}}\mathbf{B_T}(\mathbf{y}=0) = 0$, we find a peak in the magnetic field, $\mathbf{B_p}$, at $\mathbf{x} = r_p$. See Eq. (4) and Eq. (5).

$$r_p = r_x \pm r_y \tag{4}$$

$$\mathbf{B_p} = \pm\left(\frac{\mu_o I}{2\pi r_y}\right)\hat{\mathbf{y}} \tag{5}$$

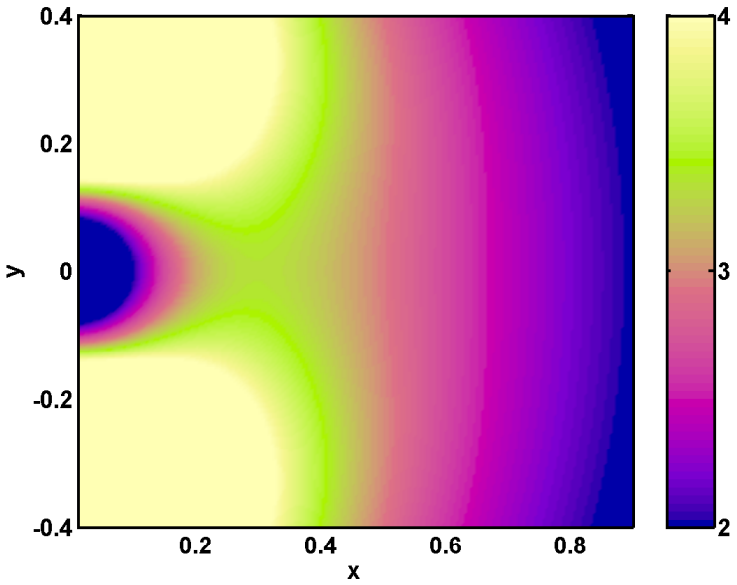

Figure 5. |B| in plane perpendicular to (2) parallel line currents (at y = ±0.3).

With only two line currents separated by a distance $2r_y$, a magnetic field profile is made with a strong peak on the $\mathbf{y} = 0$ line. The peak is displaced from the $\mathbf{x}$ location of the line currents by a distance r_y. The full 2D profile of the magnetic field due to a pair of line currents (like this example) is shown in Fig. 5. It should now be mentioned, that the magnitude of the magnetic field on the $\mathbf{y} = 0$ line is minimized, and is greater at $\pm\triangle y$. Since the $\mathbf{y} = 0$ line would likely be oriented along the discharge centerline (if it were used for the magnetic field in a Hall-effect type thruster), the increase in $\mathbf{B}$ away from $\mathbf{y} = 0$ might aid in electron confinement; it could mirror charged particles back to the discharge centerline in a manner analogous to that in a magnetic bottle.

The magnetic field in MIHA is made by the same approach, with two independent magnetic circuit elements. The elements are similar to the example given here, and shaping of the magnetic field is accomplished using ferromagnetic materials. A conventional tuning coil is used for further adjustment of the total magnetic field.

III. Experimental Apparatus

A. Prototype MIHA Thruster

A diagram of the prototype considered in this study is shown in Fig. 6. The magnetic circuit is made of grey cast iron, chosen for its magnetic permeability, and its excellent machinability. The electromagnetic circuit is wound of 1mm diameter copper magnet wire insulated with high-temperature Kapton. The use of an organic insulation precluded operation at high temperature, and restricted the peak magnetic field (to keep Joule heating to a minimum). Future windings will use ceramic or fiberglass insulation, allow a higher operating current density, and a greater peak magnetic field.

The discharge channel is Boron Nitride (BN), chosen for its high melting temperature, its relatively high thermal conductivity, and its low secondary electron emission coefficient. Macor was originally used, but proved unsuitable, since it would develop a hot spot on the side-wall opposing the $\mathbf{E} \times \mathbf{B}$ drift. After a short time the Macor side-wall would begin to melt and the discharge would become unstable. This is thought to be the result of Macor's low thermal conductivity though (an order of magnitude smaller than the thermal conductivity of BN at 1000K), and not its secondary electron emission coefficient. The channel exit is 5mm by 120mm.

Two holes were drilled in the BN channel to test different anode positions, and to test a two-anode configuration (a two-stage mode). The first is 40mm from the exit plane, and the second is 10mm from the

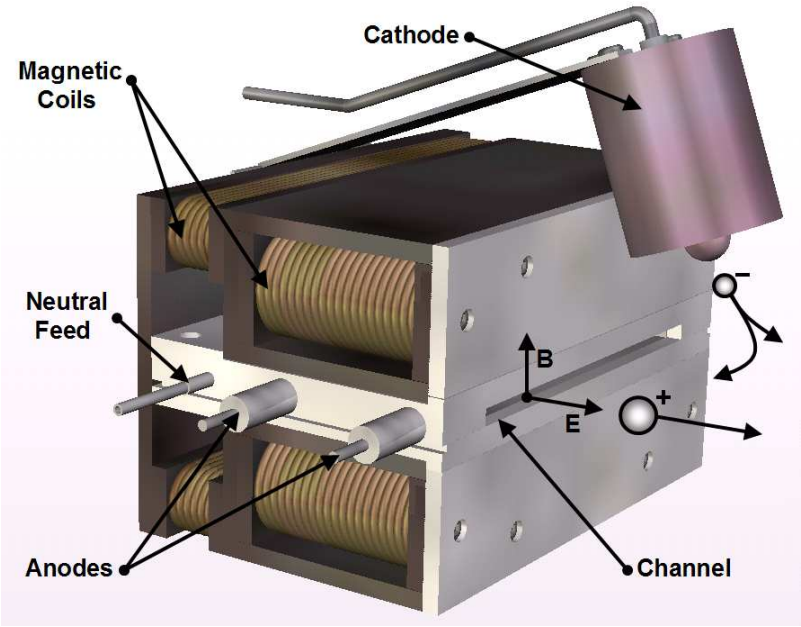

Figure 6. Diagram of linear MIHA prototype.

exit plane. Most tests occurred with a single anode though (40mm from the exit plane), since tests with a "top" stage were unsuccessful. When in use, an anode is a 2mm diameter tungsten rod at the center of the BN channel (at $\mathbf{y} = 0$). The working propellant, Xe, is delivered to channel by a 3mm diameter steel pipe. The propellant passes through (2) diffusion chambers before it enters the main discharge channel through a 100 μm slit. During all tests, there was no asymmetry in the discharge believed to result from the nonuniform injection of propellant.

The 2D magnetic field for two nominal discharge configurations is shown in Fig. 7 and Fig. 8, as calculated using the commercially available solver FEMM4.0. Independent measurements using a Hall probe indicate the error in the FE calculation to be 5% or less (on the discharge centerline). As a consequence of the Kapton insulation, the tuning coil and main coil support $\pm$2A in two different configurations. In the Negative Configuration (NC), the tuning coil creates a magnetic field in opposition to the main coil, and causes a separatrix in the magnetic field at $\mathbf{x} = -5$mm (see Fig. 7). In this case, the current in the tuning coil is represented by a negative value (-). This configuration was tested to determine whether a separatrix in the magnetic field could allow for improved ion focusing, and to see whether a reversal in the $\mathbf{E} \times \mathbf{B}$ drift could improve the thruster's performance. In the Positive Configuration (PC), the magnetic field due to the tuning coil is in the same direction as that due to the main coil (see Fig. 8), and allowed the greatest peak $\mathbf{B}$. In both configurations, the peak magnetic field increases rapidly off the discharge centerline.

B. Vacuum Facility

The experiments reported here were performed in a 4m^3 stainless steel vacuum chamber at a pressure of 1×10^{-4}Pa during nominal discharge operation (1.2 mg/s anode Xenon flow, 0.1mg/s cathode Xenon flow, and 400W discharge power). This is accomplished using a cryogenic pumping system (CVI model number TM1200) with liquid nitrogen shroud. A commercially available hollow cathode (Ion Tech HCN-252) provides the electron current necessary to sustain the discharge. The cathode is placed as shown in Fig. 6. Separate power supplies are used for the primary discharge, cathode keeper, cathode heater, and electromagnetic coils. The cathode is kept at chamber potential (ground). Measurements of the discharge current are made using a powered differential amplifier (Tektronix P5200) in parallel with a 4Ω ballast, in series with the discharge.

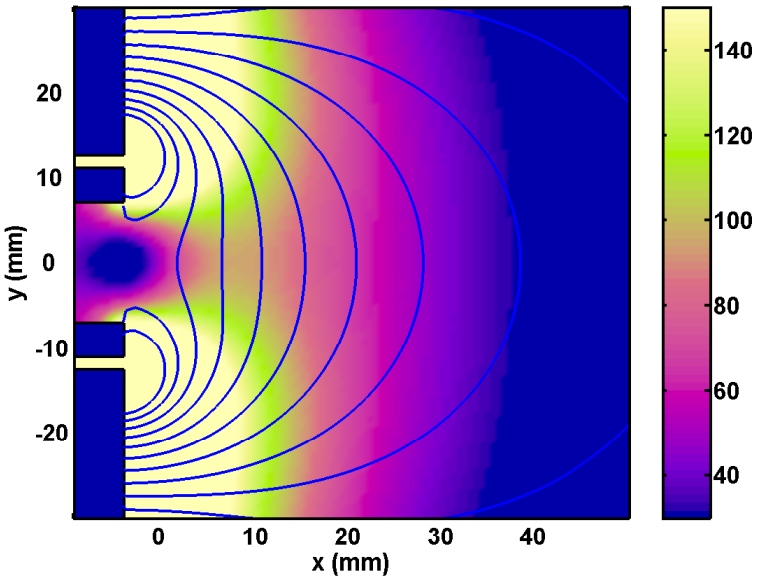

Figure 7. |B| for MIHA prototype in Gauss. NC configuration. +1A in main coil, −1A in tuning coil.

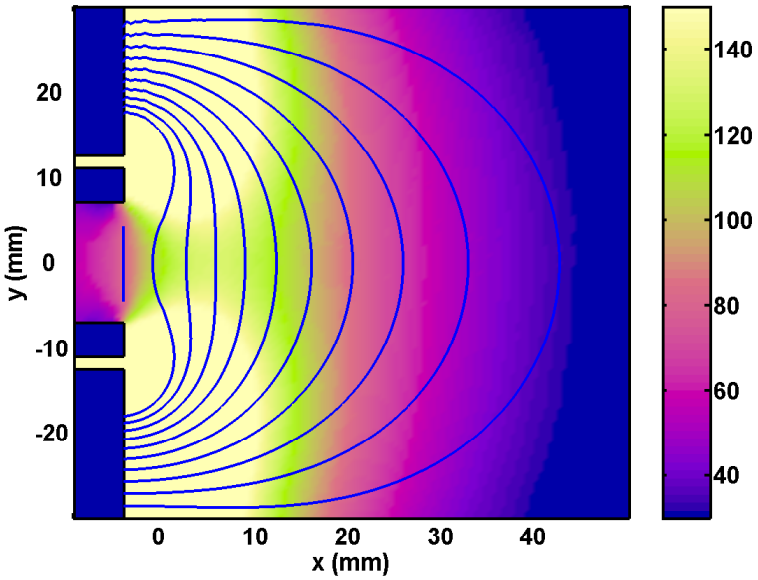

Figure 8. |B| for MIHA prototype in Gauss. PC configuration. +1A in main coil, +1A in tuning coil.

C. Thrust Stand

To measure thrust, a pendulum device is used. The prototype is placed on a mount at the top of an inverted pendulum, and the pendulum is carefully balanced. The mount is water cooled to reduce thermal drift, and electrically isolated so the MIHA prototype is allowed to float. A small amount of thrust can cause a measurable displacement of the pendulum (opposed by a spring), and the displacement is measured using a Schaevitz linear voltage differential transducer (LVDT).

To calibrate the thrust stand, the displacement of the pendulum is measured as a series of 0.5g weights is made to "pull" the pendulum (simulating thrust). Without a heat load the thrust stand provides accurate results. Unfortunately, the zero drift of the thrust stand is appreciable during nominal thruster operation, and considerable care must be taken to ensure accurate measurements. The thermal drift must be considered, and multiple measurements have to be taken (and averaged) to achieve accurate results. Due to the thermal drift, and inaccuracy in the LVDT, the accuracy of the thrust measurement is ± 0.5mN.

D. Probe Measurements

The plasma potential in the Hall thruster, Φ_p, is measured using an emissive probe. The design of the probe is based on a similar diagnostic used to investigate Russian Hall-effect thrusters in the early 1970s.[15] A thin tungsten filament is passed through the plasma plume, and the filament is heated using a floating step-down transformer connected to an AC power supply. The current in the filament is increased, increasing its temperature and its electron emissivity, until the potential of the transformer is saturated with respect to the filament current. It is then assumed that the sheath on the probe is neutralized, and the potential of the transformer is equal to the plasma potential. Other methods could have been used, but an emissive probe was preferred since it did not require the collection of an electron current. This is important since the plasma potential in the Hall-effect thruster is a sensitive function of the electron mobility, and any method that would extract electron current could modify the electron mobility. This could strongly perturb the operation of the thruster, and cause a severe error in the apparent plasma potential.

The floating potential, Φ_f, is also recorded using the emissive probe. Φ_f is defined as the potential of the transformer with no heating current, and no thermionic emission. Using a simple theory that considers the flux of charged particles to the surface of the probe, Φ_f allows a lower bound on the electron temperature, T_e, to be easily established.[16] The reason is simple; in a typical plasma, the low mass of the electron results in a high electron thermal velocity - much higher than the thermal velocity of an ion. Because of this, a body placed in a plasma will have an initial incident electron flux that is considerably higher than the incident ion flux. This causes the body to collect a negative charge, a charge that eventually reduces the incident electron flux. At equilibrium, the flux of electrons and ions to the surface is equal. In this situation, the potential of the body is called the "floating potential", and it provides information on the average electron energy - since the difference in the plasma potential and the floating potential, Φ_s, is large enough to reflect the average incident electron before it reaches the surface (see Eq. (6)).

$$\Phi_s = \Phi_p - \Phi_f \tag{6}$$

To approximate the incident electron flux at equilibrium, Γ_e, we assume the Electron Energy Distribution Function (EEDF) is Maxwellian. In this case, the electron flux is given by Eq. (7) and Eq. (8).

$$\Gamma_e = n\frac{\bar{c_e}}{4}\exp\left(\frac{q_e\Phi_s}{k_bT_e}\right) \tag{7}$$

$$\bar{c_e} = \sqrt{\frac{8}{\pi}\frac{k_bT_e}{m_e}} \tag{8}$$

In Eq. (7), the plasma number density is given by n. To approximate the ion flux, Γ_i, we assume a collisionless "free fall" sheath.[16] The ion flux is then given by Eq. (9).

$$\Gamma_i = n\sqrt{\frac{k_bT_e}{m_i}} \tag{9}$$

The electron temperature can then be approximated by Eq. (10).

$$\Phi_s = -\frac{k_e T_e}{q_e} \ln\left(\sqrt{\frac{1}{2\pi}\frac{m_i}{m_e}}\right) \tag{10}$$

The 2D map of the plasma potential and electron temperature is made using the emissive probe and a 2D translation stage. The potential of the transformer is measured using a powered differential amplifier (Tektronix P5200) connected to a Tektronix oscilloscope. This measurement is automated using LABVIEW7, so the plasma potential and floating potential is found at each point in a 20×20 grid covering 10cm×10cm.

IV. Experimental Results

A. The Top Stage

As earlier indicated, the top stage in MIHA proved difficult to operate. When on, the top stage would only function in a current limited mode ($\sim$ 2A), at a unusually low discharge voltage ($1-4$V). This result was consistently found in all tests despite considerable variation in the flowrate ($2-20$sccm) and the applied magnetic field ($0-200$G). This was unexpected, since in the Stanford SPT, 160V is needed to sustain a discharge current of 2A for 20sccm of Xe flow and a magnetic field of 100G. In combination, this suggests that the electron mobility within the discharge channel of the MIHA prototype is considerably *higher* than that in the conventional coaxial Hall accelerator, and may explain the external acceleration seen by in the Stanford Linear Thruster.[12]

It is also observed that the side-wall in the direction of the $\mathbf{E}\times\mathbf{B}$ drift is exceedingly bright, and the discharge internal to the Hall thruster is visibly asymmetric - a finding consistent with the Stanford Linear Thruster. Pending experimental confirmation, it is now hypothesized that edge effects could dominate electron transport inside the channel of a linear geometry Hall-effect thruster. It is believed that electrons drifting in the $\mathbf{E}\times\mathbf{B}$ direction can impact the side-wall. After impact with the side-wall, electrons can march along the side-wall toward the anode, colliding with the side wall at a rate comparable to the electron cyclotron frequency, Ω_e. If true, this would explain the high electron mobility within the channel, the heating of the side-wall, the asymmetry in the discharge inside the channel, and the observation of an external acceleration zone. Since the internal electron mobility is high, the potential drop inside the channel is small. This requires that the potential drop occur primarily outside the channel, where the electron mobility is comparatively small.

Since the top stage did not operate as intended, it did not provide pre-ionization of the Xe propellant, nor allow for optimization of the electrostatic potential. As a result, through the rest of this report, the operation of the MIHA prototype is given in the absence of a top stage.

B. Single Stage Operation

In a single-stage mode, the MIHA prototype behaves like a conventional Hall accelerator. It displays a strong breathing mode, the discharge current increases with the discharge voltage (generally), and the discharge current decreases if the magnetic field is increased. At a low magnetic field, the ionization efficiency is poor (as might be expected), the discharge is un-magnetized, and the plasma plume is large (see Fig. 9). In this case, the plume is purple to purple-pink, and the discharge current is high. As the magnetic field is increased the discharge becomes magnetized, the plume changes to blue to blue-white, and the extent of the plasma plume is curtailed (see Fig. 10). The discharge current decreases during this transition.

Optimum performance is realized in the PC configuration, with +2A in the main coil and +2A in the tuning coil (see Fig. 10). This is consistently found despite a battery of tests at different flow rates, and several tests with different magnetic configurations. For this reason, the results in this report concern the PC configuration seen in Fig. 10. Interestingly though, in the NC configuration, the flux to the side wall is visibly reduced (for the proper tuning coil current). According to our previous arguments regarding transport inside the discharge channel, this result could be interpreted to imply a decrease in the electron mobility within the channel, which could decrease the overall discharge current. Unfortunately, the discharge current still increased. In MIHA, the magnitude of the peak magnetic field is found to be the most important factor impacting efficiency, and not the shape of the magnetic field. Increasing the peak magnetic field (either with the main coil or the tuning coil), always decreased the discharge current. In future tests the peak current density in the magnetic coils will be increased, and each test will be repeated. It is expected that at higher $\mathbf{B}$ the profile of the magnetic field will play a greater role in the performance of the prototype.

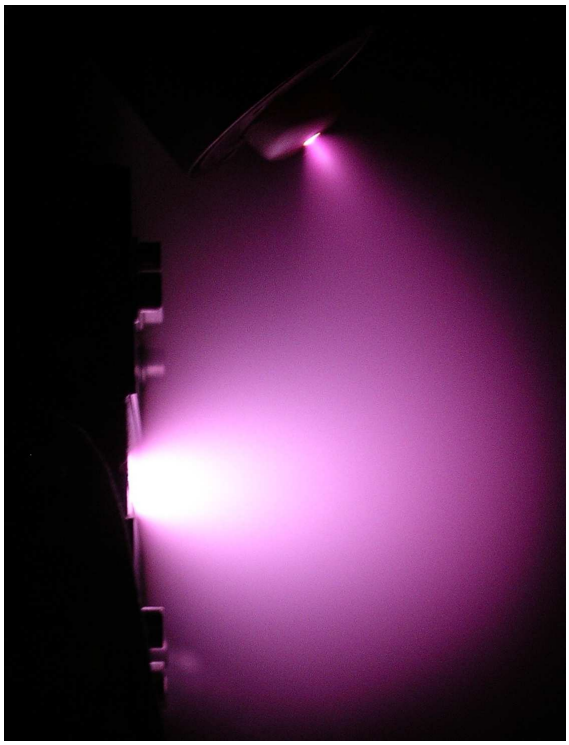

Figure 9. Prototype MIHA discharge in NC configuration. +1A in main coil, −1A in tuning coil.

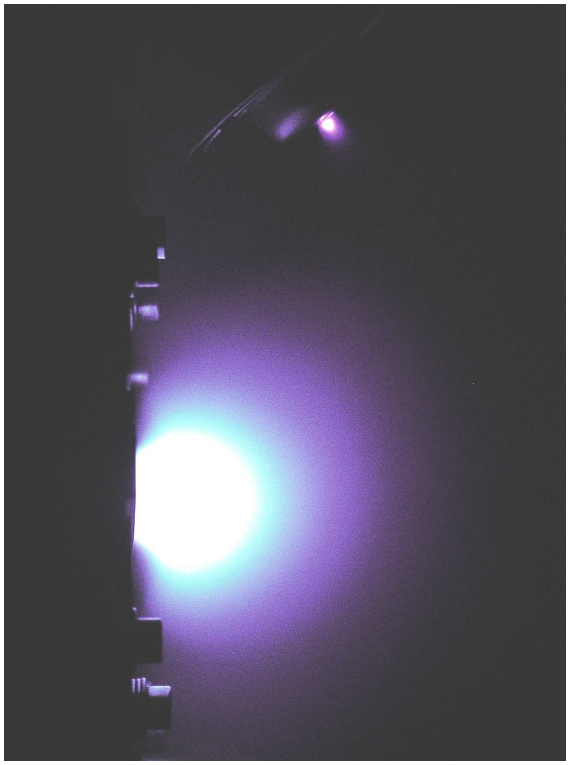

Figure 10. Prototype MIHA discharge in PC configuration. +2A in main coil, +2A in tuning coil.

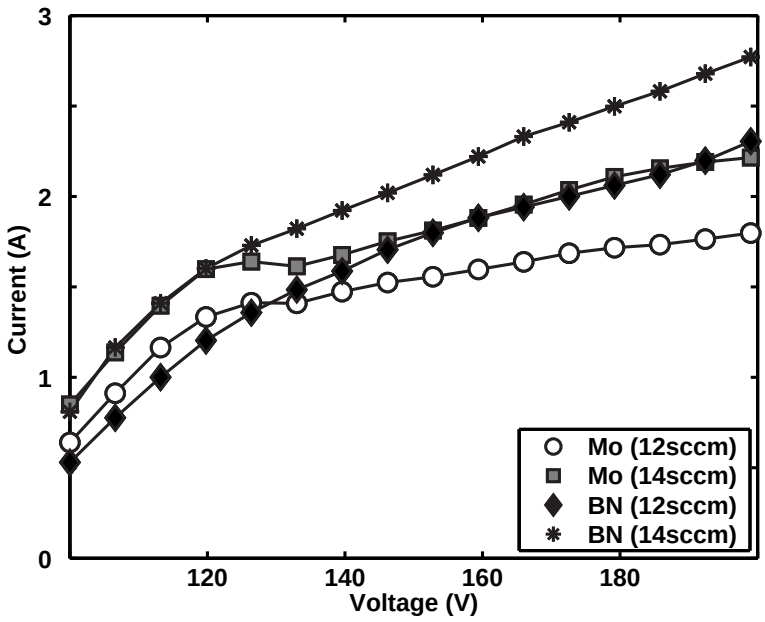

Figure 11. Prototype MIHA discharge in PC configuration. +2A in main coil, +2A in tuning coil.

Since it has been previously demonstrated that the discharge in a linear-geometry Hall-effect thruster did not depend on the channel wall material, the material covering the magnetic poles of MIHA was altered, and the impact on the discharge monitored. Boron Nitride (BN) was chosen for its secondary electron emission coefficient, and its frequent use in Hall accelerators. Molybdenum (Mo) was the second test material chosen, due to its high secondary electron emission coefficient, and its high electrical conductivity. It was thought that a weak difference between BN and Mo would demonstrate (in an extreme example) that materials have a weak impact on linear-geometry Hall accelerators.

The current-voltage characteristics are shown in Fig. 11 for both pole materials, for 12 sccm and 14 sccm of Xe flow. The discharge current is seen to increase with the discharge voltage, for both pole materials, with surprisingly linearity above 130V. Below this voltage the discharge current displays a more complicated dependence. Interestingly, a slight inflection in the discharge current for Molybdenum is seen at 130V. This inflection mimics the inflection in the same curve for BN in the Stanford SPT at the same voltage, though not to the same degree. In any case, the current-voltage characteristics do not display the level of structure seen in the same data for the Stanford SPT, and support the conjecture that the wall material and pole material do not impact the discharge in a linear-geometry Hall accelerator to a strong degree. Nevertheless, more structure is seen in Fig. 11 than in Fig. 3, and this implies that the primary body of the discharge (and the physics important to the electron mobility) occur *outside* the discharge channel of MIHA, and not inside it.

C. Oscillations

In Fig. 12 through Fig. 17, the low-frequency oscillation spectra is given for each case in Fig. 11. A strong breathing mode is seen above 130V of order 10kHz, whose sudden appearance is correlated to the linear current-voltage regime visible in Fig. 11. The frequency of the breathing mode is seen to increase with voltage, but only weakly, similar to that in a conventional Hall accelerator. It is uncertain whether the current-voltage behavior for 130-200V is a result of the observed fluctuations, or whether strong low-frequency fluctuations indicate the presence of other processes that determine the electron mobility. Interestingly, the fluctuation spectra for each case is remarkably similar, and this indicates that wall-effects are playing a weak role in the fluctuations - implying that the wall material is not a strong factor in the discharge physics.

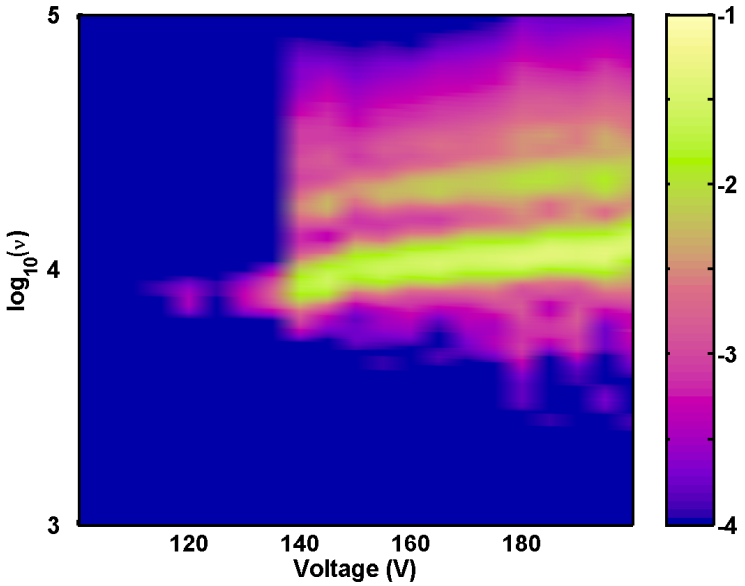

Figure 12. Discharge current fluctuation power versus voltage for BN (12sccm).

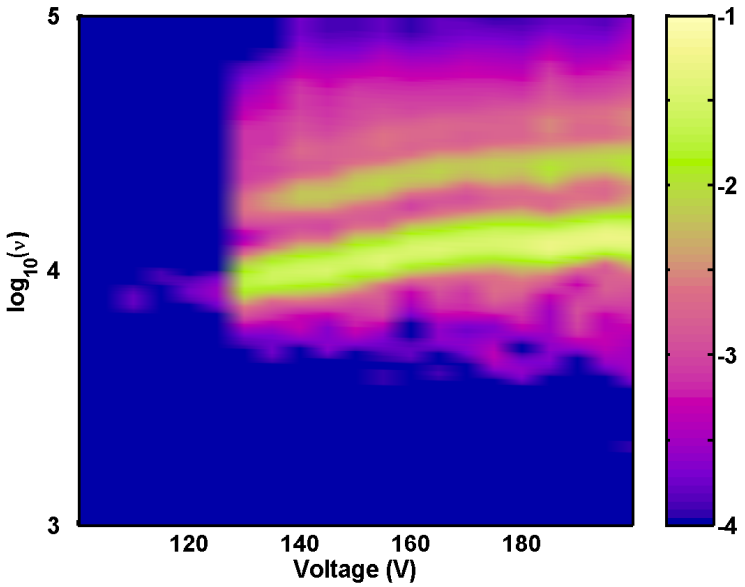

Figure 13. Discharge current fluctuation power versus voltage for BN (14sccm).

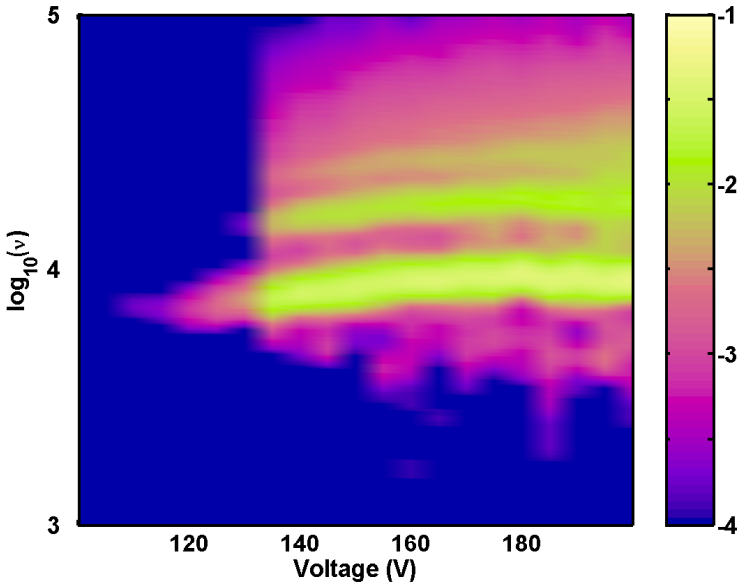

Figure 14. Discharge current fluctuation power versus voltage for Mo (12sccm).

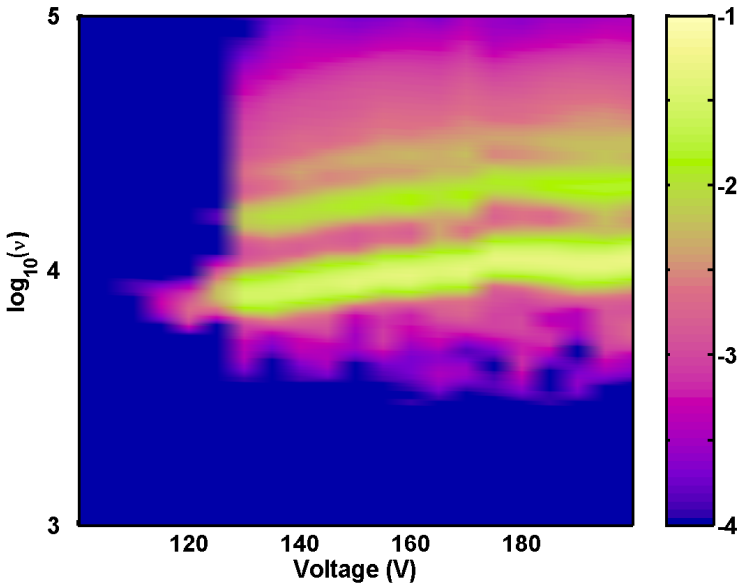

Figure 15. Discharge current fluctuation power versus voltage for Mo (14sccm).

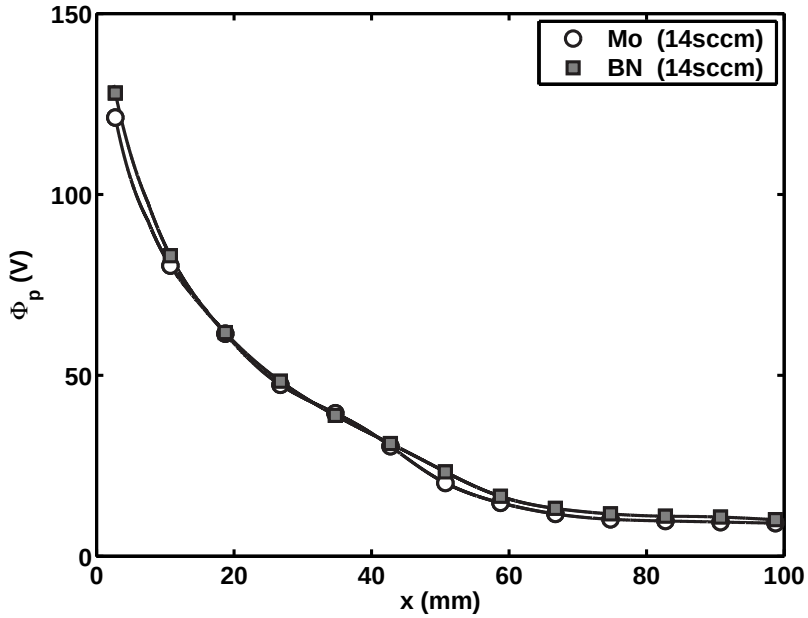

Figure 16. Plasma potential for Mo and BN cases (150V discharge, 14sccm Xe flow).

D. Plasma Potential and Electron Temperature

The plasma potential is shown for Molybdenum and Boron Nitride pole pieces at 14sccm of Xe flow. The probe data ends 2.5mm from the exit plane, since the discharge is disrupted when the probe is 1-2mm from the exit plane. This is not a surprise, and emphasizes the importance of the external discharge, and the intrusive impact of the probe. If the potential were to drop inside the channel, the probe would not be expected to cause such a dramatic impact on the discharge. As it is, the potential drops sharply outside the channel, through the entire applied potential (150V). The acceleration zone is 0-20mm outside the exit plane. For both BN and Mo, the potential profile is nearly identical, and this implies (again), that the pole material does not impact the discharge.

On a side note, it deserves mention that the movement of the probe toward the exit plane strongly affected the discharge, and as a consequence, the plasma potential measurement is likely inaccurate. The acceleration zone is outside the exit plane, but the profile of the acceleration zone is probably in error. As the probe is moved toward the exit plane, the discharge current is seen to increase by as much as 40%. Furthermore, the shape of the discharge is seen to change, and the size of the plume appears to contract, so that the most intense zone of visible radiation remains between the probe and the exit plane. In combination, these observations suggest that the acceleration zone and the body of the discharge are outside the exit plane, since if they were inside it, the discharge would not be as sensitive to an external emissive probe (like a conventional Hall accelerator).

The electron temperature is shown. The results are unremarkable, and emphasize previous conclusions. The ionization zone and the acceleration zone are outside the thruster, and the only material boundary in contact with the discharge (BN or Mo), does not impact the discharge substantially.

V. Summary

The MIHA concept is introduced, and shown to function like a conventional Hall accelerator. The peak **B**, the maximum **E**, the minimum electron mobility, and the acceleration zone, are *outside* the thruster. As a consequence, ion bombardment of the channel wall is reduced, and the wall material plays a weak role in the discharge. This could imply that the electron transport is easier to predict, but more data is necessary for this conclusion. Also, the mobility within a linear thruster is established to be unusually high, and this is a likely reason for external acceleration. Future work will refine the performance of the prototype, primarily by increasing its peak magnetic field. In addition to this, work will begin on a coaxial prototype, that should

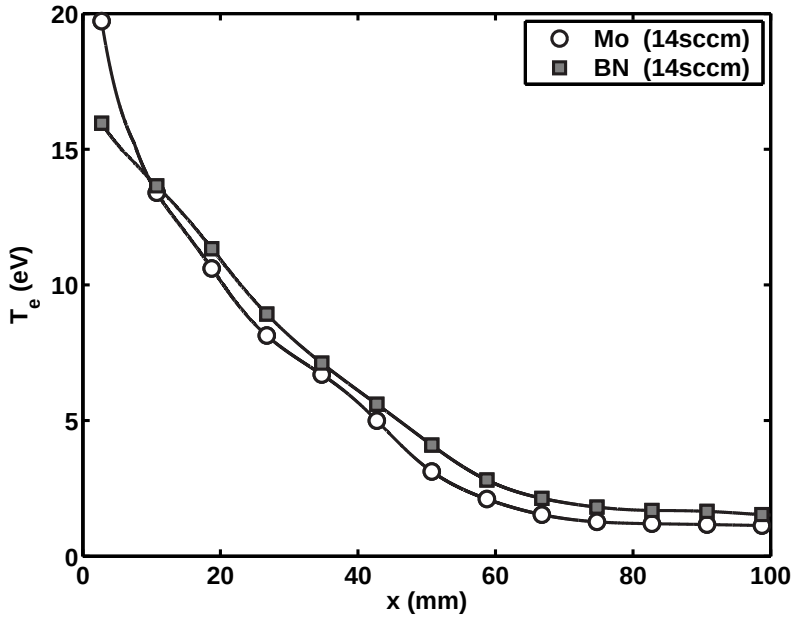

Figure 17. Electron temperature for Mo and BN cases (150V discharge, 14sccm Xe flow).

not suffer the edge-effect penalty typical of linear-geometry Hall accelerators. Further tests will continue to consider mobility in "wall-less" Hall accelerators, and attempt to determine whether the impact of the wall can be removed entirely. Lastly, erosion tests will be done to determine the effective operational life of a MIHA thruster.

Acknowledgements

Funding for this research was provided by the Air Force Office of Scientific Research. C. A. Thomas received support from the National Science Foundation, and also from Stanford University, through the Stanford University Graduate Fellowship Program.

References

[1]Zhurin, V., Kaufman, H., and Robinson, R., "Physics of closed drift thrusters," *Plasma Sources Science and Technology*, Vol. 8, No. R1, 1999.

[2]G. Hagelaar, J. Bareilles, L. G. and Boeuf, J., "Role of anomalous electron transport in a stationary plasma thruster simulation," *Journal of Applied Physics*, Vol. 93, No. 67, 2003.

[3]Fife, J., *Hybrid-PIC Modeling and Electrostatic Probe Survey of Hall Thrusters*, Ph.D. thesis, Massachusetts Institute of Technology, 1998.

[4]Bishaev, A. and Kim, V., "Local plasma properties in a Hall-current accelerator with an extended acceleration zone," *Sov. Phys. Tech. Phys.*, Vol. 23, No. 9, 1978.

[5]Hargus, W., *Investigation of the Plasma Acceleration Mechanism within a Coaxial Hall Thruster*, Ph.D. thesis, Stanford University, 2001.

[6]N. Meezan, W. H. and Cappelli, M., "Anomalous electron mobility in a coaxial Hall discharge plasma," *Physical Review E*, Vol. 63, No. 026420, 2001.

[7]D. Bohm, E. B. and Massey, H., *The Characteristics of Electrical Discharge in Magnetic Fields*, McGraw Hall, 1949.

[8]Meezan, N. and Cappelli, M., "Kinetic study of wall collisions in a coaxial Hall discharge," *Physical Review E*, Vol. 66, No. 036401, 2002.

[9]S. Barral, K. Makowski, Z. P. N. G. and Dudeck, M., "Wall material effects in stationary plasma thrusters. II. Near-wall and in-wall conductivity," *Physics of Plasmas*, Vol. 10, No. 10, 2003.

[10]N. Gascon, M. D. and Barral, S., "Wall material effects in stationary plasma thrusters. I. Paramteric studies of an SPT-100," *Physics of Plasmas*, Vol. 10, No. 10, 2003.

[11]Janes, G. and Lowder, R., "Anomalous electron diffusion and ion acceleration in a low density plasma," *Physics of Fluids*, Vol. 9, June 1966, pp. 1115–1123.

[12]N. Gascon, R. Corey, M. C. B. H., "Hall thruster with an external acceleration zone," *29th International Electric Propulsion Conference*, No. IEPC-2005-196.

[13]C. Thomas, N. G. and Cappelli, M., "Non-intrusive characterization of the hall thruster azimuthal drift current," *40th AIAA/ASME/SAE/ASEE Joint Propulsion Conference and Exhibit*, No. AIAA-2004-3776.

[14]Yioshikawa, S. and Rose, D., "Anomalous Diffusion of a Plasma accross a Magnetic Field," *Physics of Fluids*, Vol. 5, No. 334, 1962.

[15]A. Morozov, Y. Epsinchuck, A. K. V. N. and Smirnov, V., "Effect of the magnetic field on a closed-electron-drift accelerator," *Sov. Phys. Tech. Phys.*, Vol. 17, No. 482, 1972.

[16]Lieberman, A. and Lichtenberg, A., *Principles of Plasma Discharges and Materials Processing*, Wiley, 1994.